European Radiology (2019) 29:2859–2867
https://doi.org/10.1007/s00330-018-5930-0

COMPUTED TOMOGRAPHY

Radiation dose and image quality in intraoperative CT (iCT) angiography of the brain with stereotactic head frames

Robert Forbrig[1] · Lucas L. Geyer[2] · Robert Stahl[3] · Jun Thorsteinsdottir[4] · Christian Schichor[4] · Friedrich-Wilhelm Kreth[4] · Maximilian Patzig[1] · Moriz Herzberg[1] · Thomas Liebig[1] · Franziska Dorn[1] · Christoph G. Trumm[5]

Received: 9 July 2018 / Revised: 6 November 2018 / Accepted: 28 November 2018 / Published online: 11 January 2019

Abstract

Objectives Intraoperative CT (iCT) angiography of the brain with stereotactic frames is an integral part of navigated neurosurgery. Validated data regarding radiation dose and image quality in these special examinations are not available. We therefore investigated two iCT protocols in this IRB-approved study.

Methods Retrospective analysis of patients, who received a cerebral stereotactic iCT angiography on a 128 slice CT scanner between February 2016 and December 2017. In group A, automated tube current modulation (ATCM; reference value 410 mAs) and automated tube voltage selection (reference value 120 kV) were enabled, and only examinations with a selected voltage of 120 kV were included. In group B, fixed parameters were applied (300 mAs, 120 kV). Radiation dose was measured by assessing the volumetric CT dose index ($CTDI_{vol}$), dose length product (DLP) and effective dose (ED). Signal-to-noise ratio (SNR) and image noise were assessed for objective image quality, visibility of arteries and grey-white differentiation for subjective image quality.

Results Two hundred patients ($n = 100$ in each group) were included. In group A, median selected tube current was 643 mAs (group B, 300 mAs; $p < 0.001$). Median values of $CTDI_{vol}$, DLP and ED were 91.54 mGy, 1561 mGy cm and 2.97 mSv in group A, and 43.15 mGy, 769 mGy cm and 1.46 mSv in group B ($p < 0.001$). Image quality did not significantly differ between groups ($p > 0.05$).

Conclusions ATCM yielded disproportionally high radiation dose due to substantial tube current increase at the frame level, while image quality did not improve. Thus, ATCM should preferentially be disabled.

Key Points

- *Automated tube current modulation (ATCM) yields disproportionally high radiation dose in intraoperative CT angiography of the brain with stereotactic head frames.*
- *ATCM does not improve overall image quality in these special examinations.*
- *ATCM is not yet optimised for CT angiography of the brain with major extracorporeal foreign materials within the scan range.*

Keywords Brain · Radiation dosage · Neuronavigation · Computed tomography angiography

Abbreviations

ADM	Automated dose modulation
ATCM	Automated tube current modulation
$CTDI_{vol}$	Volumetric computed tomography dose index
DLP	Dose length product
ED	Effective dose
FET-PET	O-(2-^{18}F-fluoroethyl)-L-tyrosine positron emission tomography
HU	Hounsfield unit
iCT	Intraoperative computed tomography

✉ Robert Forbrig
robert.forbrig@med.uni-muenchen.de

[1] Institute of Neuroradiology, University Hospital, LMU Munich, Marchioninistrasse 15, 81377 Munich, Germany

[2] Center of Radiology and Neuroradiology, Klinikum Ingolstadt, Ingolstadt, Germany

[3] Department of Radiology, University Hospital, LMU Munich, Munich, Germany

[4] Department of Neurosurgery, University Hospital, LMU Munich, Munich, Germany

[5] Institute for Diagnostic and Interventional Radiology, Neuroradiology and Nuclear Medicine, Städtisches Klinikum München Harlaching, Munich, Germany

MAR	Metal artefact reduction
SD	Standard deviation
SNR	Signal-to-noise ratio

Introduction

Since the early 1980s, intraoperative computed tomography (iCT) of the brain has been an integral part of navigated neurosurgery [1]. Cerebral iCT is a fast, safe and robust imaging technique for both frame-based stereotactic biopsy of intracranial lesions providing tissue diagnoses with minimal disruption of anatomical structures [2–6] and intraoperative live monitoring in open neurosurgical interventions such as aneurysm clipping or resection of orbit-associated tumours [7, 8].

For stereotactic biopsy which combines stereotactic localisation and image-guided surgery, the patient's head is fixed under general anaesthesia in a stereotactic frame using an invasive fixation system [3, 6]. Then, a contrast-enhanced iCT scan is carried out, and the acquired CT images are transferred to a workstation and fused with MRI and/or O-(2-^{18}F-fluoroethyl)-L-tyrosine positron emission tomography (FET-PET) data. The target point is defined within the pathological lesion, and a possible frame-based entry point is selected without affecting neural or vascular structures by using multiplanar reconstructions.

In this setting, CT scanners should provide maximal diagnostic accuracy at a reasonable radiation dose according to the ALARA (as low as reasonably achievable) principle, which is of particular interest in young patients. Therefore, modern CT systems combine several techniques, such as automated dose modulation (ADM)—consisting of automated tube current modulation (ATCM) as a method of automatic exposure control [9–12] and automated tube voltage selection [10, 13]—as well as iterative reconstruction algorithms [14–17]. In particular, ADM allows for a reduction of image noise that is dependent on the imaged object (e.g. large patient size and foreign materials) by automatically adjusting the scanner output [18].

Until now, various studies have proven the positive effect of ADM and iterative reconstruction on radiation dose and image quality in non-contrast brain CT without foreign materials [16, 17]. With metallic implants, however, only limited experience exists in head and neck CT imaging [19–21]. Whether these techniques are effective in cerebral iCT angiography with major extracorporeal foreign materials that yield a substantial increase of image noise has not yet been systematically evaluated.

In this study, we provide data on radiation dose and image quality in stereotactic iCT angiography of the brain with and without ADM in combination with iterative reconstruction.

Methods

This retrospective single-centre study was approved by the institutional review board of the Ludwig-Maximilians-University Munich (project number: 18-200) with a waiver for written informed consent, and performed in accordance with the Declaration of Helsinki.

Neurosurgical iCT workflow

In October 2014, an intraoperative 128 slice CT scanner (Siemens SOMATOM Definition AS+, Siemens Healthineers) was installed at our institution. Cerebral iCT angiographies with stereotactic head frames for biopsy of intracranial lesions have been carried out with this CT scanner since February 2016.

For stereotactic trajectory planning, neurosurgical recommendations [3, 5, 6] on iCT are (i) whole brain imaging ranging from the skull base to vertex and (ii) visibility of intracranial landmarks such as arteries and the dedicated pathology. For metal artefact-free visualisation of the latter, the neurosurgeon usually positions the head frame either at the skull base level (in case of a supratentorial target lesion) or more cranial (in case of an infratentorial pathology). After localisation of the correct head position, the acquired CT images are then fused with the preoperatively obtained MRI and/or FET-PET, by using a dedicated planning software (e.g. iPlan and BrainLab).

Patients

In the present study, we analysed data of patients, who received a cerebral stereotactic iCT angiography for intracranial biopsy between February 2016 and December 2017.

Inclusion criteria:

- Age ≥ 18 years
- Usage of the same aluminium head frame (MHT Stereotactic Systems)
- Frame position at the level of the skull base and standardised subcutaneous fixation with four stainless steel pins (Fig. 1a–c)
- Tube voltage 120 kV

Exclusion criteria:

- Metallic implants from prior neurosurgery or neurointervention
- Non-contrast brain CT

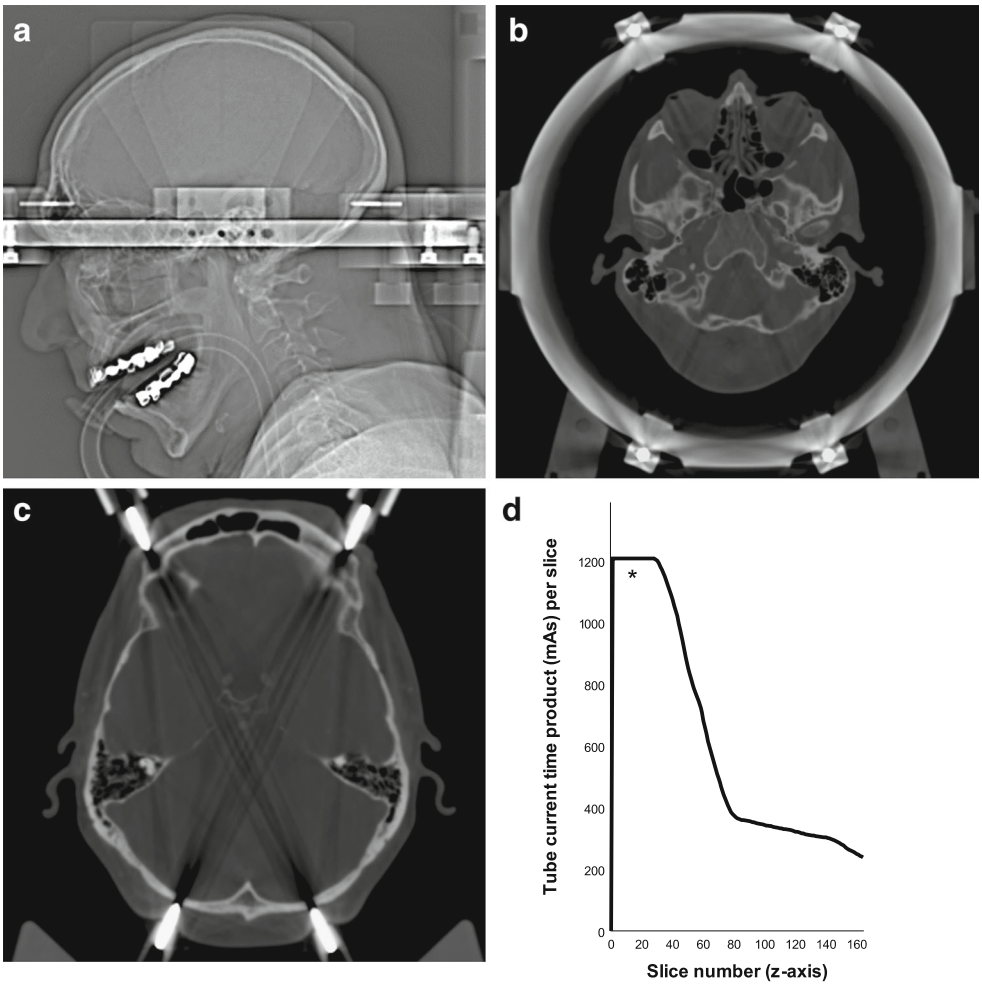

Fig. 1 Standardised position of the aluminium frame at the skull base level (lateral topogram (**a**); transversal (**b**)). **c** Streak artefacts caused by the four stainless steel fixation pins. **d** Diagram illustrating the substantial tube current increase at the frame level (*) in group A with enabled ADM (example scan length 16.4 cm, scan direction caudo-cranial)

Standardised iCT protocol

Table 1 summarises the standardised iCT acquisition protocol. After fixation of the stereotactic head frame, a topogram (i.e. localizer) was made in lateral projection. The iCT scan was acquired in caudo-cranial direction and comprised the whole neurocranium. Contrast attenuation was achieved by intravenous administration of 50 ml non-ionic iodinated contrast material (iomeprol; Imeron® 350 mg I/ml, Bracco Imaging) at a flow rate of 4.0 ml/s followed by a 50 ml saline flush. CT images were acquired in arterial phase using the bolus-tracking technique (CARE Bolus, Siemens Healthineers). In detail, a region of interest (ROI) was manually placed within the common carotid artery, and the scan started automatically after a trigger threshold of 100 Hounsfield units (HU) had been reached.

Concerning radiation dose optimisation, two different iCT protocols were applied:

A. February–December 2016: Enabled ADM, consisting of ATCM (CARE Dose 4D, Siemens Healthineers) with a preset reference value of 410 mAs and automated tube voltage selection (CARE kV, Siemens Healthineers) with a preset reference value of 120 kV as recommended by the manufacturer. This protocol was continuously applied in each iCT scan within this time span.
B. January–December 2017: Disabled ADM. During routine clinical practice, it was observed that ATCM yielded increased tube current values at the frame level. ADM was therefore disabled in January 2017 and replaced by a CT acquisition protocol with fixed tube parameters (current 300 mAs, voltage 120 kV) on a pilot basis. These tube settings yielded a favourable overall radiation dose and subjectively similar image quality when compared to the protocol with enabled ADM and were therefore maintained until the end of the study period.

For a systematic evaluation and the purpose of comparability, only those examinations in time span A with an automatically selected tube voltage of 120 kV were considered in the present study. In order to facilitate a balanced analysis of the two iCT protocols, we randomly selected 100 patients of time span, A (group A) and B (group B), each.

Images were reconstructed in axial plane with a slice thickness of 1 mm. The same iterative reconstruction algorithm (sinogram-affirmed iterative reconstruction, SAFIRE, Siemens

Table 1 Standardised iCT protocol

CT scanner	SOMATOM 128 Definition AS+ Siemens Healthineers	
Frame position	Skull base	
Topogram projection	Lateral	
Acquisition mode	Helical	
Scan direction	Caudo-cranial	
Scan range	Skull base–vertex	
Collimation	128 × 0.6 mm	
Rotation time	330 ms	
Pitch	0.55	
Contrast phase	Arterial phase (CARE Bolus)	
Contrast agent	Iomeprol 350	
Flow rate	4.0 ml/s	
Tube parameter settings	Group A	Group B
	February–December 2016 preset by the manufacturer	January–December 2017 based on own experience
Tube current	CARE Dose 4D[a]	300 mAs
Tube voltage	CARE kV[b]	120 kV
Slice reconstruction plane	Axial	
Slice thickness	1 mm	
Iterative reconstruction	SAFIRE (J30 s/3)	

[a] Quality reference value 410 mAs; [b] Quality reference value 120 kV, inclusion of all examinations with a selected voltage of 120 kV. *iCT*, intraoperative computed tomography; *SAFIRE*, sinogram-affirmed iterative reconstruction

Healthineers) with a recommended strength of 3 was used in both groups. After completion of the examination, image data and dose reports were transferred to a dedicated workstation (syngo.via, Siemens Healthineers) and picture archiving and communication system (syngo Imaging, Siemens Healthineers).

Radiation dose analysis

Individual values of automatically selected tube current in group A as well as the volumetric CT dose index ($CTDI_{vol}$), dose length product (DLP) and acquisition length in both groups were recorded from the patient protocols. The effective dose (ED) estimate was calculated by multiplying the DLP with a head-specific conversion coefficient k of 0.0019 mSv/[mGy cm] [22] according to the ICRP 103 publication [23].

Objective image analysis

Regarding objective image analysis, a neuroradiologist with 8 years of experience in diagnostic neuroradiology (R.F.) calculated signal-to-noise ratio (SNR) and image noise of the grey and white matter outside the frame level by using a dedicated picture archiving and communication system software (syngo Imaging, Siemens Healthineers). In detail, ROIs with a size of 20–30 mm^2 were placed manually within the caudate nucleus and posterior limb of the internal capsule, as described by other authors [16]. The mean attenuation value (HU) and standard deviation (SD) within a ROI were defined as signal and image noise, respectively (MW and SD in Fig. 2). The SNR was then calculated as signal divided by image noise. To minimise the effect of discordant values, the respective measurements were carried out three times and averaged for each region.

Subjective image analysis

All examinations were independently reviewed in random order by two radiologists with 8 (R.F.) and 4 (M.H.) years of experience in diagnostic neuroradiology. The readers were blinded to the two groups, and window settings were freely adjustable. Subjective image quality was analysed both within and outside the frame level with focus on the two parameters 'grey-white differentiation' and 'arteries', by using a three-point scale (0 = poor/non-diagnostic, 1 = sufficient, 2 = good).

Statistics

Data analysis was performed using IBM SPSS Statistics for Windows, Version 24.0 (IBM Corp.). Data were initially assessed for normality applying the Kolmogorov-Smirnov test. The paired t test was used to compare gender and patient age between groups A and B, with values shown as mean ± standard deviation (range). The Mann-Whitney U test was applied to compare acquisition length, radiation dose, objective image quality and subjective image quality between groups, with values shown as median (25–75%

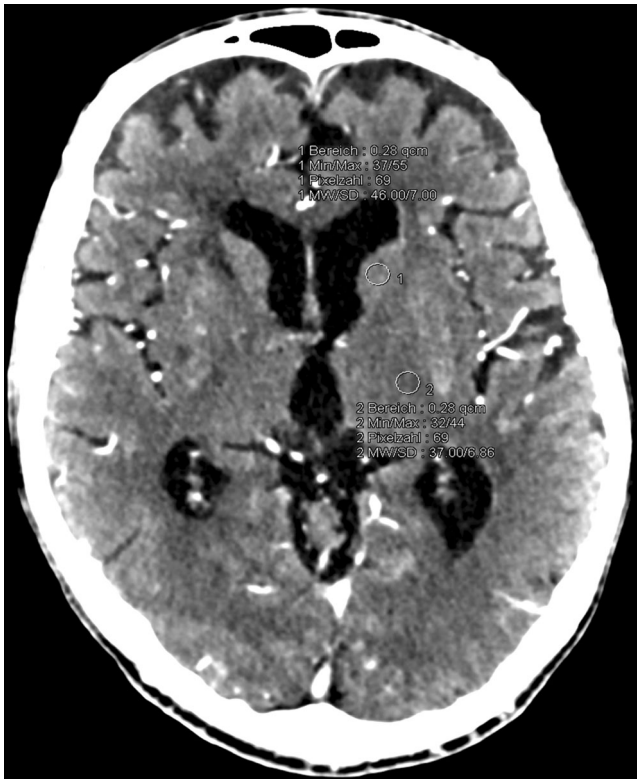

Fig. 2 Example of objective image analysis with manually placed ROIs within the caudate nucleus and posterior limb of the internal capsule. The illustrated values for the grey and white matter are ROI size 28 mm^2, mean signal (MW) 46 HU and 37 HU and image noise (SD) 7. Based on these measurements, the SNR of the grey and white matter is 6.6 and 5.3

interquartile range). A level of significance of $\alpha = 0.05$ was used throughout the study.

Results

Table 2 gives an overview of patient characteristics. Of the 200 patients, 84 were female and 116 male. The mean patient age was 63 years (range, 18–84 years). Differences of gender and patient age between groups did not reach statistical significance ($p > 0.05$).

Table 2 Patient characteristics

	Group A ADM enabled	Group B ADM disabled	*p* value
No. of patients	100	100	
Male/female	56/44	60/40	0.569
Age, years[a]	62.6 ± 14.9 (18–79)	64.1 ± 12.8 (22–84)	0.157

[a] Data are shown as mean ± standard deviation (range). *ADM*, automated dose modulation; *No.*, number

Radiation dose

Radiation dose values of both groups are shown in Table 3. Median acquisition lengths were 15.7 cm (15.1–16.5 cm) in group A and 16.6 cm (15.7–17.5 cm) in group B ($p < 0.001$).

In group A, the median tube current was 643 mAs (624–656 mAs; fixed value in group B, 300 mAs; $p < 0.001$). Within and outside the frame level, median tube current values in group A were 1207 mAs (1054–1207 mAs) and 332 mAs (304–364 mAs) ($p < 0.001$) (Fig. 1d).

Median overall values of $CTDI_{vol}$ and DLP were 91.54 mGy (88.40–94.29 mGy) and 1561 mGy cm (1497–1665 mGy cm) in group A, and 43.15 mGy (43.15–43.15 mGy) and 769 mGy cm (732–809 mGy cm) in group B ($p < 0.001$).

ED values were significantly higher ($p < 0.001$) in group A with a median value of 2.97 mSv (2.84–3.16 mSv) in comparison to group B with a median value of 1.46 mSv (1.39–1.54 mSv). The parameters of group B yielded an ED reduction of 51% compared to group A.

Objective image quality

Objective image quality did not significantly differ between groups (Table 3; $p > 0.05$). In group A, the median SNR of the grey and white matter was 6.2 (5.9–6.6) and 4.8 (4.4–5.3), respectively, in comparison to 6.1 (5.8–6.7) and 4.9 (4.5–5.1) in group B, respectively. In both groups, median image noise was equally 8 SD HU (7–8) in the grey matter and 7 SD HU (7–8) in the white matter.

Subjective image quality

There was no significant difference in subjective image quality ($p > 0.05$) (Fig. 3**)**. Within and outside the frame level, two readers rated the parameter 'grey-white differentiation' exclusively as 0 and 2, respectively, for both groups. Regarding the parameter 'arteries' within the frame level, the median rating of the two observers was 1 (1–1) for both groups. In brain regions outside the frame level, this parameter was equally rated 2 for each patient in both groups.

Discussion

The main finding of the present study is that ATCM resulted in significant increase of tube current at the frame level, with peak values of more than 1000 mAs per slice. Consequently, overall values of commonly applied dose descriptors ($CTDI_{vol}$, DLP and ED) were significantly higher in the group with enabled ADM when compared to the group with disabled ADM. It is a fact that the use of automatic exposure control may vary (i.e. decrease or increase) $CTDI_{vol}$ depending on the

Table 3 Radiation dose and objective image quality of groups A and B

	Group A ADM enabled	Group B ADM disabled	*p* value
Radiation dose			
Aquisition length (cm)	15.7 (15.1; 16.5)	16.6 (15.7; 17.5)	< 0.001
Tube current (mAs)	643 (624; 656)	300 (fixed value)	< 0.001
$CTDI_{vol}$ (mGy)	91.54 (88.40; 94.29)	43.15 (43.15; 43.15)	< 0.001
DLP (mGy cm)	1561 (1497; 1665)	769 (732; 809)	< 0.001
ED (mSv)	2.97 (2.84; 3.16)	1.46 (1.39; 1.54)	< 0.001
Objective image quality			
SNR GM	6.2 (5.9; 6.6)	6.1 (5.8; 6.7)	0.858
Image noise GM	8 (7; 8)	8 (7; 8)	0.652
SNR WM	4.8 (4.4; 5.3)	4.9 (4.5; 5.1)	0.649
Image noise WM	7 (7; 8)	7 (7; 8)	0.475

Data are shown as median (25%; 75% interquartile range). *ADM*, automated dose modulation; *$CTDI_{vol}$*, volumetric computed tomography dose index; *DLP*, dose length product; *ED*, effective dose; *SNR*, signal-noise-ratio; *GM*, grey matter; *WM*, white matter

imaged object and noise [18]. However, the study by Bier et al [20] demonstrated that the use of ATCM in cerebral CT angiographies at 120 kV can work effectively even in patients with metallic implants (e.g. aneurysm clips and coils), resulting in a remarkably lower radiation dose (mean ED 0.84 mSv) compared to our study. Note, in the present study, the ED increase in the group with enabled ADM was measured despite using lateral topograms for iCT angiography planning. It has been shown that lateral topograms usually yield both a higher image quality and lower radiation dose in CT

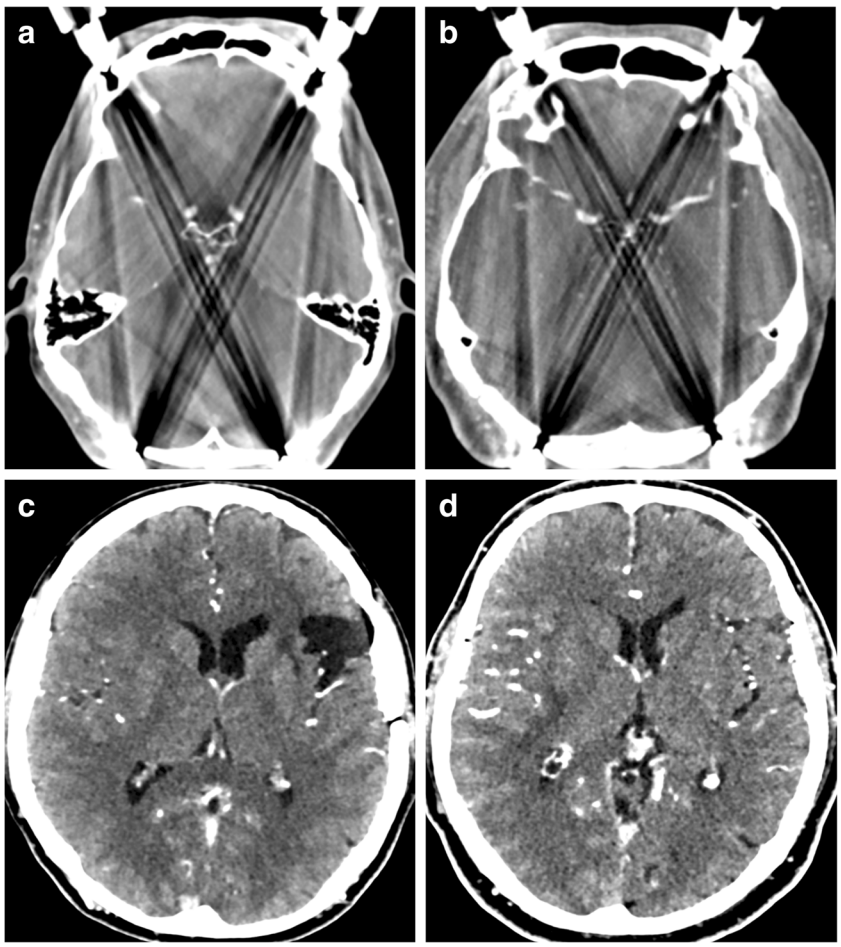

Fig. 3 Subjective image analysis of the parameters 'arteries' and 'grey-white differentiation'. At the level of the frame fixation pins, the large brain-supplying arteries can be identified sufficiently in both groups despite severe streak artefacts, whereas the grey-white differentiation is not detectable (group A, ADM enabled (**a**); group B, ADM disabled (**b**)). Outside the frame plane, the two parameters are clearly visible in both groups (group A, ADM enabled (**c**); group B, ADM disabled (**d**))

examinations with enabled ATCM when compared to anterior-posterior topograms [24], even though it is not yet clear if these results are valid for head CT studies. Altogether, our data suggest that ATCM is not yet optimised for cerebral CT angiographies with major extracorporeal foreign materials within the scan range such as stereotactic head frames. Thus, ATCM should preferentially be disabled in these special examinations until further notice. Furthermore, as the automatic exposure control system applied in the present study uses a combined ATCM technique (CARE Dose 4D, Siemens Healthineers) which considers the patient's size and attenuation changes [9], it is particularly useful for body parts that are not uniform in size (e.g. chest and abdomen) [10, 11], and its strength in brain CT is rather limited.

In the group with disabled ADM, we chose a fixed tube current of 300 mAs and tube voltage of 120 kV. These values are within the normal range for cerebral CT angiographies [20, 25, 26]. Consequently, radiation dose in the group with disabled ADM was—in contrast to the group with enabled ADM—clearly below the diagnostic reference level of brain CT provided by the respective federal office for radiation protection ($CTDI_{vol}$ = 60 mGy, DLP = 850 mGy cm) [27] and comparable to results of another cerebral CT angiography study that did not specifically examine patients with foreign materials but used ATCM [26]. In addition to optimising tube current, the value of decreasing tube voltage has been investigated by recent studies on cerebral CT angiography; lowering the tube voltage to 70 kV, ideally in combination with a reduced amount of iodinated contrast agent, allows for a reduction in ED of up to 85% with a simultaneous increase in SNR [26, 28–30]. In the present study, the tube voltage was not decreased, because the image noise in consideration of the head frame might have been too severe, which in turn could possibly lead to a significant decrease of overall image quality. In summary, we believe that our fixed tube settings, which are also a prerequisite for the present study, may be a reasonable compromise in these particular CT examinations with major extracorporeal foreign materials within the scan range.

In contrast to others [20, 21, 26, 28], we did not assess the SNR of intracranial arteries; measurement of intra-arterial signal attenuation was neither reliable at the level of the circle of Willis due to frame-associated metal artefacts nor in the distal segments due to partial volume effects. Nevertheless, according to Guziński et al [16], representative artefact-free values of SNR and image noise at the level of the basal ganglia could be obtained. The calculations of both parameters were comparable to others [26] and statistically equal in both groups.

Subjective image quality outside the frame plane was rated as equally good in both groups. Within the frame level, grey-white differentiation was neither detectable in the group with enabled nor in the group with disabled ADM, whereas landmark structures such as arteries were sufficiently visible in both groups. These findings indicate that ATCM did not improve image quality despite significant increase of tube current at the frame level as described above. Regarding the latter, dedicated metal artefact reduction (MAR) techniques such as iterative algorithms [19, 20], interpolation with filtered back projection [31], adaptive filtering [32] or dual energy CT [33] might improve image quality. For example, it has been shown that the iterative algorithm iMAR (Siemens Healthineers) can minimise artefacts caused by deep brain stimulation electrodes [19] as well as aneurysm clips and coils [20]. However, as the region of interest—i.e. the intracranial pathology and the adjacent arteries—was located outside this level and clearly visible in each patient, the neurosurgeon did not need detailed anatomical information within the frame level. Furthermore, MAR itself may induce other, previously unfamiliar artefacts [20, 34].

In our standard iCT angiography protocol, SAFIRE strength 3 was automatically preset by the manufacturer. It has been demonstrated that this iterative reconstruction algorithm reduces both image noise and partial volume effects, particularly when using a thin slice acquisition [15]. As CT images of both groups were reconstructed with a slice thickness of 1 mm, the advantage of SAFIRE utilised in both groups was equally effective. In this context, it is worth referring to Chen GZ et al [26] who suggested that SAFIRE strength 4 should be preferentially used in cerebral CT angiography, even though the tube voltage was set to 70 kV in their study.

Our results have to be evaluated in light of several study limitations. Firstly, we did not perform dosimetric measurements in the present study; thus, objective data on the actual patient radiation dose—in particular at the head frame level—are missing. However, according to published data of other authors who carried out dosimetric measurements on a thorax phantom with extracorporeal metallic shielding [35], we believe that the excess radiation at the frame level caused by ATCM will not be fully absorbed by the metallic material, consequently yielding increased patient radiation dose at this level. Secondly, only one specific algorithm from one vendor was used for ATCM (CARE Dose 4D, Siemens Healthineers), and the efficacy of alternative algorithms from other manufacturers in these particular examinations is unknown. To confirm our findings, we therefore recommend phantom measurements (that also represent the reference standard for radiation dose estimation) with the same metal immobilisation device as used for stereotactic iCT on a few other CT scanner models. Thirdly, the standardly applied head frame in this study was made of aluminium, and the fixation pins were composed of stainless steel. Alternative materials with potentially lower x-ray absorption (e.g. carbon) might have improved the efficacy of ATCM. Finally, MAR algorithms were not implemented. However, these algorithms usually affect the image quality, but not the radiation dose. Furthermore, as mentioned above, the neurosurgeon does not need detailed anatomical information within the frame level for stereotactic biopsy planning.

In conclusion, in the present study, ATCM yielded a disproportionally high radiation dose caused by a substantial increase of tube current at the frame level. However, this escalation of the radiation dose had no diagnostic benefit, and the image quality remained reduced at the frame level. According to our data, we therefore assume that ATCM is not yet optimised for brain CT angiography with major extracorporeal foreign materials within the scan range. Further research will be required to obtain more detailed information on the exact patient dose delivery. Until then, ATCM should preferentially be disabled in these special examinations. In comparison, CT examinations with fixed tube parameters (120 kV, 300 mAs) yielded a favourable overall patient radiation dose and equally good image quality in the brain regions outside the frame level which are of primary interest for the stereotactic neurosurgeon.

Acknowledgements Part of the data was presented orally at the ECR 2018 in Vienna, Austria, and the XXI Symposium Neuroradiologicum 2018 in Taipei, Taiwan.

Funding The authors state that this work has not received any funding.

Compliance with ethical standards

Guarantor The scientific guarantor of this publication is PD Dr. Christoph G. Trumm.

Conflict of interest The authors of this manuscript declare no relationships with any companies, whose products or services may be related to the subject matter of the article.

Statistics and biometry PD Dr. Robert Stahl kindly provided statistical advice for this manuscript.

Informed consent Written informed consent was waived by the Institutional Review Board.

Ethical approval Institutional Review Board approval was obtained.

Methodology
- retrospective
- diagnostic study
- performed at one institution

References

1. Shalit MN, Israeli Y, Matz S, Cohen ML (1982) Experience with intraoperative CT scanning in brain tumors. Surg Neurol 17:376–382
2. Can SM, Turkmenoglu ON, Tanik C et al (2017) Computerized tomography-guided stereotactic biopsy of intracranial lesions: report of 500 consecutive cases. Turk Neurosurg 27:395–400
3. Kreth FW, Muacevic A, Medele R, Bise K, Meyer T, Reulen HJ (2001) The risk of haemorrhage after image guided stereotactic biopsy of intra-axial brain tumours–a prospective study. Acta Neurochir (Wien) 143:539–545
4. Rachinger W, Grau S, Holtmannspötter M, Herms J, Tonn JC, Kreth FW (2009) Serial stereotactic biopsy of brainstem lesions in adults improves diagnostic accuracy compared with MRI only. J Neurol Neurosurg Psychiatry 80:1134–1139
5. Eigenbrod S, Trabold R, Brucker D et al (2014) Molecular stereotactic biopsy technique improves diagnostic accuracy and enables personalized treatment strategies in glioma patients. Acta Neurochir (Wien) 156:1427–1440
6. Grasbon-Frodl EM, Kreth FW, Ruiter M et al (2007) Intratumoral homogeneity of MGMT promoter hypermethylation as demonstrated in serial stereotactic specimens from anaplastic astrocytomas and glioblastomas. Int J Cancer 121:2458–2464
7. Schichor C, Rachinger W, Morhard D et al (2010) Intraoperative computed tomography angiography with computed tomography perfusion imaging in vascular neurosurgery: feasibility of a new concept. J Neurosurg 11:722–728
8. Terpolilli NA, Rachinger W, Kunz M et al (2016) Orbit-associated tumors: navigation and control of resection using intraoperative computed tomography. J Neurosurg 124:1319–1327
9. Söderberg M, Gunnarsson M (2010) Automatic exposure control in computed tomography–an evaluation of systems from different manufacturers. Acta Radiol 51:625–634
10. Sabel BO, Buric K, Karara N et al (2016) High-pitch CT pulmonary angiography in third generation dual-source CT: image quality in an unselected patient population. PLoS One 11:e0146949
11. Wichmann JL, Hardie AD, Schoepf UJ et al (2017) Single- and dual-energy CT of the abdomen: comparison of radiation dose and image quality of 2nd and 3rd generation dual-source CT. Eur Radiol 27:642–650
12. De Cecco CN, Darnell A, Macías N et al (2013) Second-generation dual-energy computed tomography of the abdomen: radiation dose comparison with 64- and 128-row single-energy acquisition. J Comput Assist Tomogr 37:543–546
13. Spearman JV, Schoepf UJ, Rottenkolber M et al (2016) Effect of automated attenuation-based tube voltage selection on radiation dose at CT: an observational study on a global scale. Radiology 279:167–174
14. Geyer LL, Schoepf UJ, Meinel FG et al (2015) State of the art: iterative CT reconstruction techniques. Radiology 276:339–357
15. Haubenreisser H, Fink C, Nance JW Jr et al (2014) Feasibility of slice width reduction for spiral cranial computed tomography using iterative image reconstruction. Eur J Radiol 83:964–969
16. Guziński M, Waszczuk Ł, Sąsiadek MJ (2016) Head CT: image quality improvement of posterior fossa and radiation dose reduction with ASiR - comparative studies of CT head examinations. Eur Radiol 26:3691–3696
17. Wenz H, Maros ME, Meyer M et al (2016) Intra-individual diagnostic image quality and organ-specific-radiation dose comparison between spiral cCT with iterative image reconstruction and z-axis automated tube current modulation and sequential cCT. Eur J Radiol Open 3:182–190
18. Christner JA, Braun NN, Jacobsen MC, Carter RE, Kofler JM, McCollough CH (2012) Size-specific dose estimates for adult patients at CT of the torso. Radiology 265:841–847
19. Aissa J, Boos J, Schleich C et al (2017) Metal artifact reduction in computed tomography after deep brain stimulation electrode placement using iterative reconstructions. Invest Radiol 52:18–22
20. Bier G, Bongers MN, Hempel JM et al (2017) Follow-up CT and CT angiography after intracranial aneurysm clipping and coiling-improved image quality by iterative metal artifact reduction. Neuroradiology 59:649–654

21. Morsbach F, Wurnig M, Kunz DM et al (2013) Metal artefact reduction from dental hardware in carotid CT angiography using iterative reconstructions. Eur Radiol 23:2687–2694
22. Deak PD, Smal Y, Kalender WA (2010) Multisection CT protocols: sex- and age-specific conversion factors used to determine effective dose from dose-length product. Radiology 257:158–166
23. (2007) The 2007 recommendations of the International Commission on Radiological Protection. ICRP publication 103. Ann ICRP 37:1–332
24. Suntharalingam S, Wetter A, Guberina N et al (2016) Impact of the scout view orientation on the radiation exposure and image quality in thoracic and abdominal CT. Eur Radiol 26:4072–4079
25. Takeyama N, Kuroki K, Hayashi T et al (2012) Cerebral CT angiography using a small volume of concentrated contrast material with a test injection method: optimal scan delay for quantitative and qualitative performance. Br J Radiol 85:e748–e755
26. Chen GZ, Zhang LJ, Schoepf UJ et al (2015) Radiation dose and image quality of 70 kVp cerebral CT angiography with optimized sinogram-affirmed iterative reconstruction: comparison with 120 kVp cerebral CT angiography. Eur Radiol 25:1453–1463
27. Federal Office for Radiation Protection (2016) Publication of updated diagnostic reference levels for diagnostic and interventional X-ray examinations [Article in German]. Federal Office for Radiation Protection, Berlin. Available via http://www.bfs.de/SharedDocs/Downloads/BfS/DE/fachinfo/ion/drw-roentgen.pdf?__blob=publicationFile&v=9. Accessed 23 Oct 2018
28. Chen Y, Zhang X, Xue H et al (2017) Head and neck angiography at 70 kVp with a third-generation dual-source CT system in patients: comparison with 100 kVp. Neuroradiology 59:1071–1081
29. Ni QQ, Chen GZ, Schoepf UJ et al (2016) Cerebral CTA with low tube voltage and low contrast material volume for detection of intracranial aneurysms. AJNR Am J Neuroradiol. https://doi.org/10.3174/ajnr.A4803
30. Chen GZ, Fang XK, Zhou CS, Zhang LJ, Lu GM (2017) Cerebral CT angiography with iterative reconstruction at 70kVp and 30mL iodinated contrast agent: initial experience. Eur J Radiol 88:102–108
31. Yu L, Li H, Mueller J et al (2009) Metal artifact reduction from reformatted projections for hip prostheses in multislice helical computed tomography: techniques and initial clinical results. Invest Radiol 44:691–696
32. Kachelriess M, Watzke O, Kalender WA (2001) Generalized multi-dimensional adaptive filtering for conventional and spiral single-slice, multi-slice, and cone-beam CT. Med Phys 28:475–490
33. Meinel FG, Bischoff B, Zhang Q, Bamberg F, Reiser MF, Johnson TR (2012) Metal artifact reduction by dual-energy computed tomography using energetic extrapolation: a systematically optimized protocol. Invest Radiol 47:406–414
34. Wuest W, May MS, Brand M et al (2015) Improved image quality in head and neck CT using a 3D iterative approach to reduce metal artifact. AJNR Am J Neuroradiol 36:1988–1993
35. Coursey C, Frush DP, Yoshizumi T, Toncheva G, Nguyen G, Greenberg SB (2008) Pediatric chest MDCT using tube current modulation: effect on radiation dose with breast shielding. AJR Am J Roentgenol 190:W54–W61